Aerodynamic Models of Complicated Constructions Using Parallel Smoothed Particle Hydrodynamics

Alexander Titov, Sergey Khrapov, Victor Radchenko and Alexander Khoperskov✉

Volgograd State University, Volgograd, Russia
khoperskov@volsu.ru

Abstract. In current paper we consider new industrial tasks requiring of air dynamics calculations inside and outside of huge and geometrically complicated building constructions. An example of such constructions are sport facilities of a semi-open type for which is necessary to evaluate comfort conditions depending on external factors both at the stage of design and during the further operation of the building. Among the distinguishing features of such multiscale task are the considerable size of building with a scale of hundreds of meters and complicated geometry of external and internal details with characteristic sizes of an order of a meter. Such tasks require using of supercomputer technologies and creating of a 3D-model adapted for computer modeling. We have developed specialized software for numerical aerodynamic simulations of such buildings utilizing the smoothed particle method for Nvidia Tesla GPUs based on CUDA technology. The SPH method allows conducting through hydrodynamic calculations in presence of large number of complex internal surfaces. These surfaces can be designed by 3D-model of a building. We have paid particular attention to the parallel computing efficiency accounting for boundary conditions on geometrically complex solid surfaces and on free boundaries. The discussion of test simulations of the football stadium is following.

Keywords: Computational Fluid Dynamics · Nvidia Tesla · CUDA · Smooth Particle Hydrodynamics · Multiscale Modeling

1 Introduction

The supercomputer methods qualitatively enhance our capabilities in the design of complex and non-standard constructions. The determination of aerodynamic fields in the immediate vicinity of the object and study of possible environment impacts on it or its parts are the main aims of many studies. One of the most powerful tools in studying of the aerodynamic properties of projected constructions are the wind tunnel experiments [1]. However, the huge sizes, complexity of constructions and lack of hydrodynamic similarity in some cases limit the possibilities of such approach [2].

Here we list several tasks for which numerical gas-dynamic simulations for building constructions seem necessary. For the effective and safe missiles launching it is very important to determine the shock-wave loads on the launcher and other surrounding objects [3, 4]. Technical improvements of design of the missile body, launch container, ballistic missile silo launcher requires the analysis of gas-dynamic and shock-wave processes at missile launch [3, 5]. The problem complicates in the case of above-water or submerged missile launches [6]. Examples of outstanding applied scientific achievements are technologies of computational aerodynamics of moving objects in the field of missile construction [7], aircraft building [8–10], design of cars and other land transport [11–13].

The interaction with air flow should be accounted for in practice of design and building of large constructions. The calculation of wind load for high-rise buildings or the entire microdistrict with complex landscape features is an independent problem [14]. An important trend in the development of such models connects with calculations of wind loads on new architectural solutions with complex free geometry [15]. In all tasks listed above the main aim is the definition of the strength characteristics of the constructions.

In current paper, we notice another class of industrial problems requiring of air motion calculation outside and inside of complex and very large constructions depending on meteorological conditions. Sport stadiums of a semi-open type can be a good example due to the need of comfortable conditions creation depending on external factors. And we have to solve such problem at the design stage. The task is similar to the determination of the air motion inside of large industrial buildings, where a variety of technological equipment is the source of flows [16, 17]. The differences are caused with scales of the computational domain and determinant influence of external meteorological factors in our case. The massive transition of numerical algorithms and parallel software to GPUs is a modern trend [18]. Thus, that is our key aim as well.

2 Aerodynamic numerical model

2.1 Mathematical model

We consider the problem of calculating the velocity field inside and outside a complex large structure, depending on the wind regime, air temperature. The gas compressibility calculation for the complete system of gas dynamics equations, gravity and vertical inhomogeneity of the density ϱ, pressure p, entropy $s \propto \ln(p/\varrho^\gamma)$ allows us to model convective instability when necessary conditions arise. We use the equations of hydrodynamics in the following form:

$$\frac{\partial \varrho}{\partial t} + \nabla(\varrho \mathbf{U}) = 0\,, \quad \frac{\partial \mathbf{U}}{\partial t} + (\mathbf{U}\nabla)\mathbf{U} = -\frac{\nabla p}{\varrho} + \mathbf{g}\,, \quad \frac{\partial \varepsilon}{\partial t} + \mathbf{U}\nabla\varepsilon + \frac{p}{\varrho}\nabla\mathbf{U} = 0\,, \quad (1)$$

where ϱ is the gas mass density, $\mathbf{U} = \{u_x; u_y; u_z\}$ is the velocity vector, $\nabla = \{\partial/\partial x; \partial/\partial y; \partial/\partial z\}$, $|\mathbf{g}| = 9.8\,\mathrm{m{\cdot}s^{-2}}$, p is the pressure, ε is the internal energy.

The thermodynamic parameters are related by the equation of state of an ideal gas

$$p = \frac{\varrho}{\mu}\mathcal{R}T \quad \text{or} \quad \varepsilon = \frac{p}{(\gamma - 1)\,\varrho}\,, \tag{2}$$

where $\mathcal{R}$ is the ideal gas constant, $\gamma = 1.4$ is the adiabatic index, $\mu = 29\,\mathrm{g/mol}$ is air the molar mass, and T is the temperature. The standard gas impenetrable boundary conditions should been set on solid surfaces.

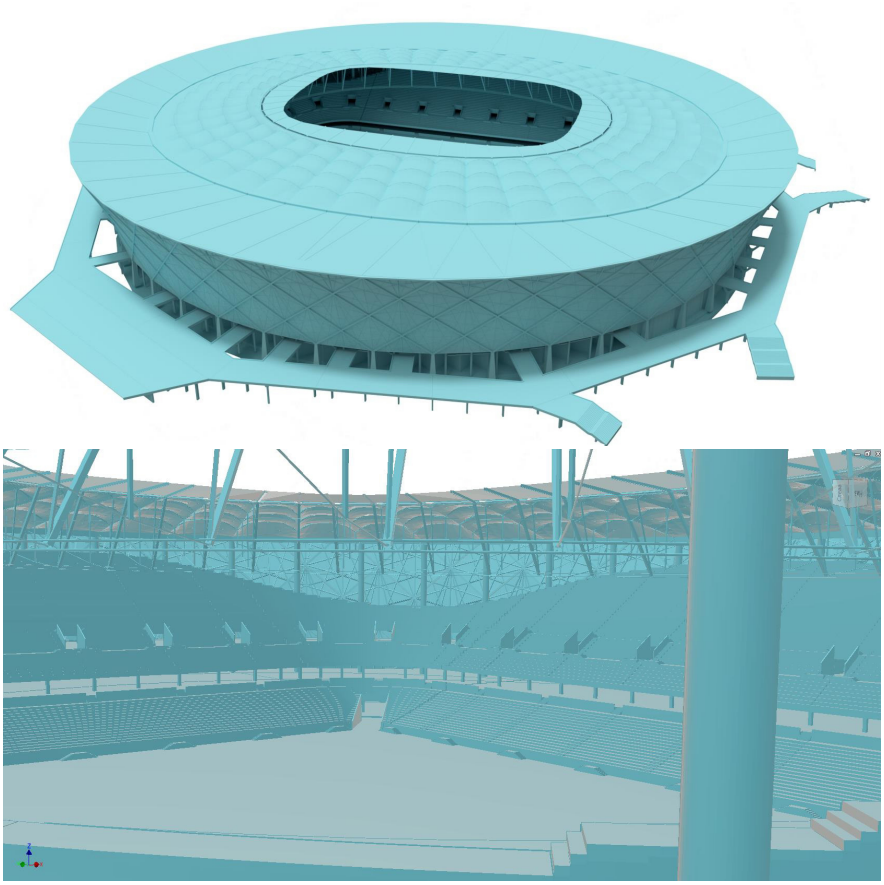

Fig. 1. The common view of the 3D stadium model is shown from the outside (top) and inside (bottom)

2.2 3D-model of construction

The construction complexity is caused by the large number of different passways, the complex geometry of internal system of storey and stairways, the tribunes

and the adjoining terrain (Figure 1). We set the boundary conditions on the gas-dynamic functions at all solid surfaces, thus the quality of the aerodynamic model is substantially defined by the accuracy of reproduction of construction structural features.

We propose using of the standard technologies of 3D modeling of solids, for which powerful software tools exist. The key idea is a 3D model created at the stage of building design using the drawings in the formats .dwg, .dxf, .pdf, etc. The spatial accuracy of such model lies within the range $0.01 - 0.1$ m. The 3D model includes all design features of the construction, internal partitions, passways to the interior rooms, tribunes and field (See Figure 1).

The further consideration and all the test calculations have been carried out for the football stadium model of the Volgograd-Arena type. The original accurate high-resolution 3D-model requires adaptation for aerodynamic modeling. Our task is concordance of the design parameters with the SPH model resolution taking into the account the finite particle radius h. In our 3D-model we have removed the smallest girders, columns and structural details (see Figure 1b) for hydrodynamic simulations.

Using standard 3D modeling methods in Blender the spatial volume for all building elements such as roof, storeys, internal stairways and tribunes have been assigned. All components were combined into a single 3D model by Boolean operations. Finally, a particular attention has been paid to the modeling of through passways to the field and tribunes, on which air flows significantly affect. The working format of the 3D model is *.stl.

2.3 Boundary conditions

Using of fixed particles along a solid surface is one of the methods of solid boundaries modeling in SPH approach [19, 20]. Particles are placed on a boundary or inside a solid body depending on a distance between confining surfaces and radius of particle, h. These Fixed Particles have all the properties of gas particles (density, energy, pressure), but their velocity is zero and they always remain at their initial positions. Recalculation of density and energy at each time step increases the calculation accuracy in the vicinity of solid surfaces. Such fixed particles take part in the through calculation ensuring the parallelization efficiency.

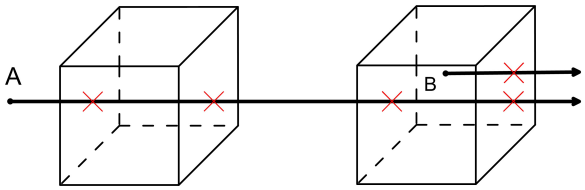

Fig. 2. The distribution of Fixed Particles by the raytracing method

Our specially written Python script for Blender provides the Fixed Particles configuration formation. We use an algorithm based on ray tracing determining whether a point belongs to a complex object (Figure 2). In 3D model the parity of number of planes intersections is verified by an arbitrary ray for a particle at the point A or B (see Figure 2). The function returns "False" in case of an even number of intersections and "True" for an odd number of intersections.

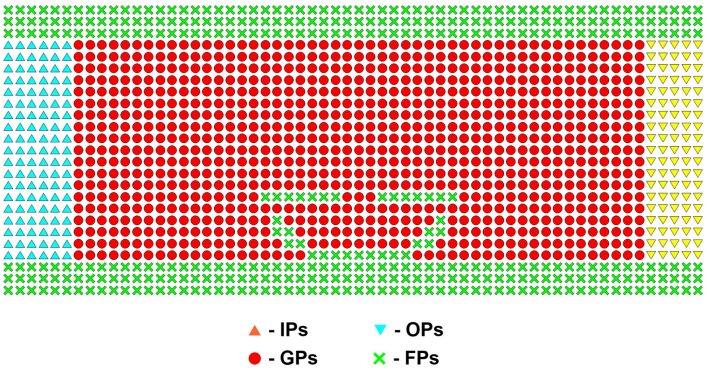

Fig. 3. The SPH particles types and the configuration of the computational domain

To model the wind flow in a Cartesian coordinates along the x-coordinate, we set free boundary conditions on the left and right side of the computational domain (see Figure 3). It is convenient to define different wind directions $\mathbf{V}_a$ by a corresponding rotation of the 3D-model in a fixed coordinate system. We introduce three additional types of particles (IPs, OPs and DPs) to realize the free boundary conditions ensuring the inflow/outflow of air into the computational domain. As a result, our model contains five types of particles: Gaseous Particles (GPs), Fixed Particles (FPs), Outflow Particles (OPs), Inflow Particles (IPs), Dead Particles (DPs).

The inflow region at free boundary (left part of Figure 3) consists of several layers of uniformly distributed IPs particles. For such particles all the gas dynamic parameters are fixed and the condition $\mathbf{U}_i = \mathbf{V}_a$ fulfills for their velocity until the moment then the particle crosses the inflow region. After the particle coming into the outflow zone it moves with constant velocity and fixed parameters (at the right side of Figure 3). When the particle leaves the outflow region through the right border and ceases to affect the GPs it receives the "Dead Particle" status (Figure 4).

2.4 The numerical model for the GPU

The SPH approach asserts wide opportunities for computational code parallelization for a variety of applications using GPUs. Using specially developed

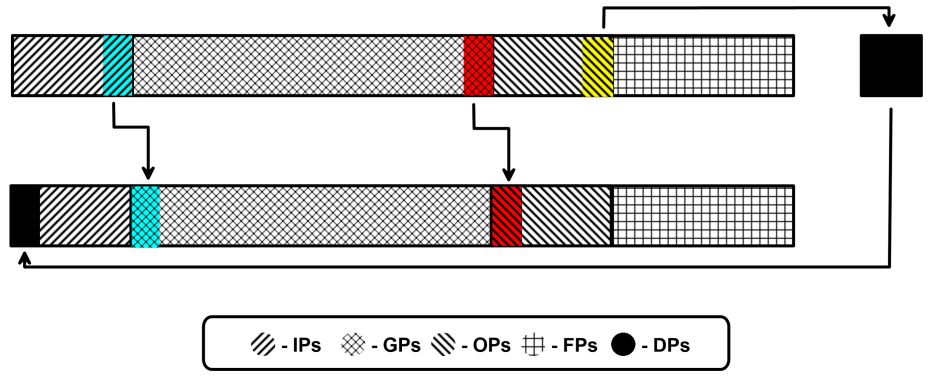

Fig. 4. The redistribution of particles of different types for free boundaries

algorithms for solving the resource-intensive problem of N-bodies [21, 22] the wonderful results were obtained for astrophysical flows [23, 24]. The SPH method evinces considerable capabilities for modeling the dynamics of liquid free surface in the Earth's gravitational field [25].

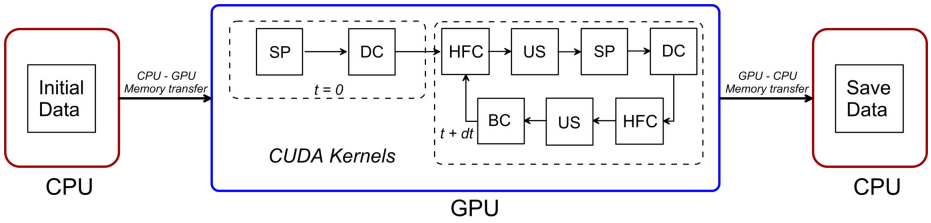

Fig. 5. Flow diagram for the parallel code

The program written for problem solve from Ref. [22] without self-gravitation which accounts for new conditions of our task has been our base of program code. The boundary conditions are calculated in the CUDA BC (Boundary Conditions) kernel, while presence of different particle types is accounted in the CUDA SP (Sorting Particles), DC (Density Calculating), HFC (Hydrodynamics Forces Calculating) and US (Update Systems) kernels (Figure 5). BC CUDA block consists of two CUDA-kernels:
1) kernelInsert_Dead$<<<N/BlockSize, BlockSize>>>$ indexes particles that have left the calculation domain (DPs).
2) kernelAdd_Inflow$<<<(Nin+BlockSize-1)/BlockSize, BlockSize>>>$ creates a new layer of Inflow Particles from the Dead Particles.

The corresponding snippet of code is shown below.

The code for CUDA-core: kernelInsertDead and kernelAdd_inflow

```
__global__ void kernelInsert_Dead(int*
                SPH_newinflow_ind, int* type, int *count)
{
        int i = threadIdx.x + blockIdx.x * blockDim.x;
        if (type[i] == type_dead) {
                int ndx = atomicAdd(count, 1);
                SPH_newinflow_ind[ndx] = i;
        }
}
__global__ void kernelAdd_Inflow(int* SPH_newinflow_ind,
                    Real4* Pos, Real4* Vel, Real4* Post,
                    Real4* Velt, Real2* Mass_hp, int* type)
{       int i = threadIdx.x + blockIdx.x * blockDim.x;
        if (i < dd.N_inflow) {
                int ndx = SPH_newinflow_ind[i];
                int kz = i / dd.Ny_inflow;
                int ky = i - kz * dd.Ny_inflow;
                Real x = dd.x_inflow;
                Real y = dd.y_inflow + ky * dd.step;
                Real z = dd.z_inflow + kz * dd.step;
                Pos[ndx].x = x;  Pos[ndx].y = y;  Pos[ndx].z = z;
    Update_Particles_Characteristics(Pos, Vel, Post, Velt,
                                     Mass_hp, type);
        }
}
```

The efficiency rise of an algorithm of the nearest neighbor search is an important direction in the parallel SPH-method development [26]. For the nearest neighbor search the hierarchical grids and cascading particle sorting algorithm have been applied using the partial sums parallel calculation in SP CUDA kernels. The sorting algorithm have been specified in Ref. [22]. Figure 6 shows the corresponding common scheme of the nearest neighbor search for the SPH method.

The analysis reveals that a relative contribution of the SP and BC CUDA kernels to the overall SPH algorithm runtime is less than 0.3 %. The latter indicates the efficiency of the parallel implementation of these CUDA kernels. We analyzed the scalability of computations on models with different number of particles N and for different Nvidia Tesla GPUs (Table 1). The memory of the GPU K20 is not enough for calculation with $N = 2^{25}$. Our SPH algorithm uses only global memory, so increasing the runtime of Cuda kernels by 1.7 times can be explained by more efficient access to global memory on the K80 compared to the K40. The memory bandwidth is 480 Gbit / s on K80 and 288 Gbit / sec on K40.

We tested the code on standard problems, for example, the decay of an arbitrary pressure discontinuity with the formation of a shockwave, a rarefaction

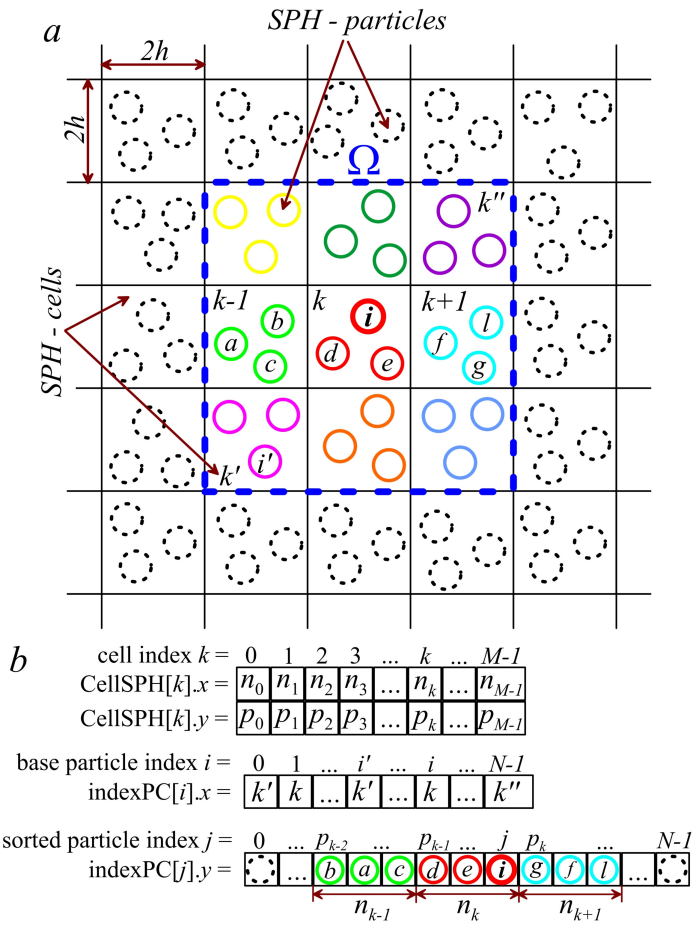

Fig. 6. The scheme of the nearest-neighbor search. a) The distribution of SPH particles in grid cells. Ω is the subdomain determining the i-th particle interaction with neighboring particles. b) The arrays for sorting particles (M is the number of cells, n_k is the number of particles at the k-th cell, $p_k = \sum_{l=0}^{k} n_l$, and N is total number of particles.

Table 1. The execution time of CUDA kernels on GPUs $[t_{SPH}]$ = sec, $[Memory]$ =Gb.

	$K20$ (1GPU)		$K40$ (1GPU)		$\frac{1}{2} \times K80$ (1GPU)	
$N \times 1024$	t_{SPH}	$Memory$	t_{SPH}	$Memory$	t_{SPH}	$Memory$
4096	6.02	0.618	4.95	0.618	2.47	0.618
32768	–	–	69.2	6.243	41.6	6.243

wave and a contact discontinuity, the gas flow from the vessel into the vacuum through a small hole, Couette flow, and others.

2.5 Simulation results and discussion

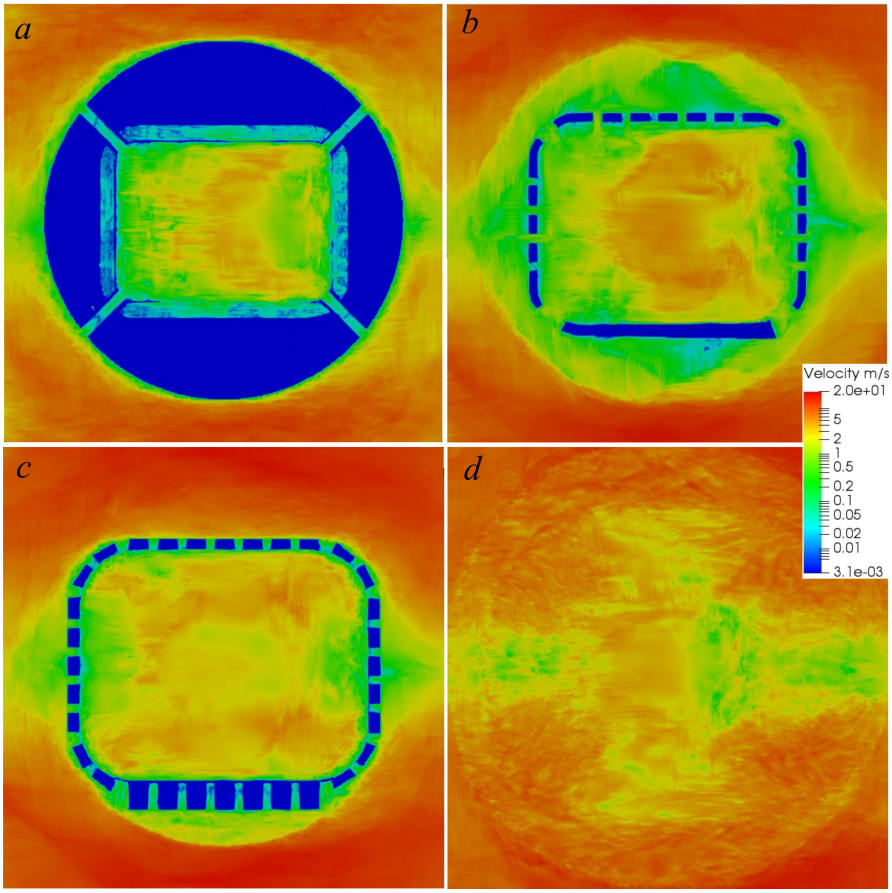

Fig. 7. The distribution of the velocity modulus at different heights above the football field level: a) the ground level layer, $z = 2$ m, b) at the second-floor height, $z = 12$ m, c) under the roof $z = 21$ m, d) above the roof $z = 40$ m.

We have considered the structure of the wind flow on the Volgograd-Arena stadium 3D-model (see § 2.2). The velocity and direction of wind, $\mathbf{V}_a$, the SPH particle radius, h, the number of particles, N have been test parameters to determine the efficiency and quality of our numerical model. Figure 7 represents the flow structure in the xOy plane for different heights z in the model with the particles number $N = 2^{25}$.

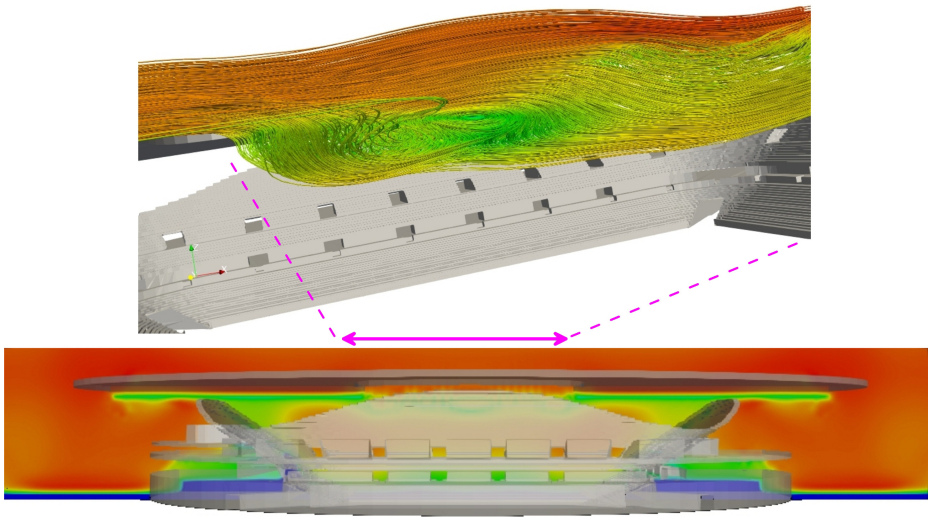

Fig. 8. The vertical flow pattern ($|\mathbf{U}(x,z)|$). The insert shows the flow structure in vicinity of the roof. The vortices below the roof plane are clearly visible.

The flow pattern in the vertical plane is presented in Figure 8, where the vortex structures are seen in the vicinity of the roof inner edges above the football field.

The SPH approach advantages are the following.
1) The manufacturability of constructing of the aerodynamic models due to the 3D-model of the building, which is always built at the building design stage and the best way describes the real object.
2) The boundary conditions specification is simple on solid surfaces and free boundaries and provides better parallelization in comparison with grid methods.
3) The SPH approach disclose incredible prospects for structural components elastic movements modeling under the influence of the wind flow.

The air mobility inside of open and semi-open sport facilities is determined by external meteorological factors and strongly depends on direction and velocity of wind and convective state of an atmosphere. The application fields of such aerodynamic models are connected with operation features of sport facilities. We highlight separately the security measures of spectators and participants of sport events caused by flying insects problem, which is relevant for the Volgograd-Arena, the Rostov-Arena and other stadiums in the southern regions during the spring-summer period. We can conduct an expert examination of the efficiency of various methods of technical protection, for example the usage of special ventilation and aspiration devices to reduce insects penetration into the stadium separately for passively spreading insects (such as imago midges) and actively flying insects (such as mosquitoes). The main advantage of the SPH method for our problem is a simple procedure for specifying solids using the 3D model of a structure instead of generating 3D meshes with a complex topology.

Acknowledgments. We used the results of numerical simulations carried out on the supercomputers of the Research Computing Center of M.V. Lomonosov Moscow State University. AK and SK are grateful to the Ministry of Education and Science of the Russian Federation (government task No. 2.852.2017/4.6). VR is thankful to the RFBR (grants 16-07-01037).

References

1. Egorychev O.O., Orekhov G.V., Kovalchuk O.A., Doroshenko S.A. Studying the design of wind tunnel for aerodynamic and aeroacoustic tests of building structures. Scientific Herald of the Voronezh State University of Architecture and Civil Engineering. Construction and Architecture. 2012. no.4, 7-12 (2012)
2. Sun X., Liu H., Su N., Wu Y. Investigation on wind tunnel tests of the Kilometer skyscraper. Engineering Structures. 148, 340-356 (2017)
3. Peshkov R.A., Sidel'nikov R.V. Analysis of shock-wave loads on a missile, launcher and container during launches. Bulletin of the South Ural State University. Ser. Mechanical Engineering Industry. 15, 81-91 (2015)
4. Kravchuk M.O., Kudryavtsev V.V., Kudryavtsev O.N., Safronov A.V., Shipilov S.N., Shuvalova T.V. Research on Gas Dynamics of Launch in Order to Ensure the Development of Launching Gear for the Angara A5 Rocket at Vostochny Cosmodrome. Cosmonautics and Rocket Engineering. 7 (92), 63-71 (2016)
5. Fu D., Hao H. Investigations for Missile Launching in an Improved Concentric Canister Launcher. J. of Spacecraft and Rockets. 52, 1510-1515 (2015)
6. Yang J., Feng J., Li Y., Liu A., Hu J., Ma Z. Water-exit process modeling and added-mass calculation of the submarine-launched missile. Polish Maritime Research. 24, 152-164 (2017)
7. Dongyang C., Abbas L.K., Rui Xiaoting R., Guoping W. Aerodynamic and static aeroelastic computations of a slender rocket with all-movable canard surface. Proceedings of the Institution of Mechanical Engineers, Part G: Journal of Aerospace Engineering. 232, 1103-1119 (2017)
8. Liang Y., Ying Z., Shuo Y., Xinglin Z., Jun D. Numerical simulation of aerodynamic interaction for a tilt rotor aircraft in helicopter mode. Chinese J. of Aeronautics. 29(4), 843-854 (2016)
9. Lv H., Zhang X., Kuang J. Numerical simulation of aerodynamic characteristics of multielement wing with variable flap. Journal of Physics: Conference Series. 916, 012005 (2017)
10. Guo N. Numerical Prediction of the Aerodynamic Noise From the Ducted Tail Rotor. Engineering Letters. 26, 187-192 (2018)
11. Janosko I., Polonec T., Kuchar P., Machal P., Zach M. Computer Simulation of Car Aerodynamic Properties. Acta Universitatis Agriculturae et Silviculturae Mendelianae Brunensis. 65, 1505-1514 (2017)
12. Janson T., Piechna J. Numerical analysis of aerodynamic characteristics of a of high-speed car with movable bodywork elements. Archive of Mechanical Engineering. 62, 451-476 (2015)
13. Saad S., Hamid M.F. Numerical study of aerodynamic drag force on student formula car. ARPN J. of Engineering and Applied Sciences. 11, 11902-11906 (2016)
14. Zhang Z., Sien M., To A., Allsop A. Across-wind load on rectangular tall buildings. The Structural Engineer. 95, 36-41 (2017)

15. Jendzelovsky N., Antal R., Konecna L. Determination of the wind pressure distribution on the facade of the triangularly shaped high-rise building structure. MATEC Web of Conferences. 107, 00081 (2017)
16. Butenko M., Shafran Yu., Khoperskov S., Kholodkov V., Khoperskov A. The optimization problem of the ventilation system for metallurgical plant. Applied Mechanics and Materials. 379, 167-172 (2013)
17. Averkova O.A., Logachev K.I., Gritskevich M.S., Logachev A.K. Ventilation of Aerosol in a Thin-Walled Suction Funnel with Incoming Flow. Part 1. Development of Mathematical Model and Computational Algorithm. Refractories and Industrial Ceramics. 58, 242-246 (2017)
18. Kopysov S., Kuzmin I., Nedozhogin N. Novikov N., Sagdeeva Y. Scalable hybrid implementation of the Schur complement method for multi-GPU systems. J. of Supercomputing. 69, 81-88 (2014)
19. Monaco A.D., Manenti S., Gallati M., Sibilla S., Agate G., Guandalini R. SPH Modeling of Solid Boundaries Through a Semi-Analytic Approach. Engineering Applications of Computational Fluid Mechanics. 5, 1-15 (2011)
20. Valizadeh A., Monaghan J.J. A study of solid wall models for weakly compressible SPH. J. of Computational Physics. 300, 5-19 (2015)
21. Bedorf J., Gaburov E., Zwart S.P. A sparse octree gravitational N-body code that runs entirely on the GPU processor. J. of Computational Physics. 231, 2825-2839 (2012)
22. Khrapov S., Khoperskov A. Smoothed-particle hydrodynamics models: implementation features on GPUs. Communications in Computer and Information Science. 793, 266-277 (2017)
23. Buruchenko S.K., Schafer C.M., Maindl T.I. Smooth Particle Hydrodynamics GPU-Acceleration Tool for Asteroid Fragmentation Simulation. Procedia Engineering. 204, 59-66 (2017)
24. Khrapov S.S., Khoperskov S.A., Khoperskov A.V. New features of parallel implementation of N-body problems on GPU. Bulletin of the South Ural State University, Ser.: Mathematical Modelling, Programming and Computer Software. 11, 124-136 (2018)
25. Afanas'ev K.E., Makarchuk R.S. Calculation of hydrodynamic loads at solid boundaries of the computation domain by the ISPH method in problems with free boundaries. Russian J. of Numerical Analysis and Mathematical Modelling. 26, 447-464 (2011)
26. Winkler D., Rezav M., Rauch W. Neighbour lists for smoothed particle hydrodynamics on GPUs. Computer Physics Communications. 225, 140-148 (2017)